1521-0103/370/3/894–901$35.00
THE JOURNAL OF PHARMACOLOGY AND EXPERIMENTAL THERAPEUTICS

https://doi.org/10.1124/jpet.118.255372
J Pharmacol Exp Ther 370:894–901, September 2019

The Journal of PHARMACOLOGY And Experimental Therapeutics

Special Section on Drug Delivery Technologies

A Polymeric Nanogel-Based Treatment Regimen for Enhanced Efficacy and Sequential Administration of Synergistic Drug Combination in Pancreatic Cancer[S]

Kruti S. Soni,[1] Divya Thomas, Thomas Caffrey, Kamiya Mehla, Fan Lei, Kelly A. O'Connell, Satish Sagar, Subodh M. Lele, Michael A. Hollingsworth, Prakash Radhakrishnan, and Tatiana K. Bronich

Department of Pharmaceutical Sciences, Center for Drug Delivery and Nanomedicine, College of Pharmacy (K.S.S., F.L., T.K.B.), Eppley Institute for Research in Cancer and Allied Diseases, Fred and Pamela Buffett Cancer Center (D.T., T.C., K.M., K.A.O., S.S., M.A.H., P.R.), and Department of Pathology and Microbiology (S.M.L.), University of Nebraska Medical Center, Omaha, Nebraska

Received November 27, 2018; accepted January 15, 2019

ABSTRACT

Pancreatic ductal adenocarcinoma (PDAC) is one of the most lethal cancers. A combination of cisplatin (CDDP) and gemcitabine (Gem) treatment has shown favorable clinical results for metastatic disease; both are limited by toxicities and nontargeted delivery. More than 80% of PDAC aberrantly expresses the sialyl Tn (STn) antigen due to the loss of function of the core 1β3-Gal-T–specific molecular chaperone, a specific chaperone for the activity of core 1 β3-galactosyltransferase or C1GalT. Here, we report the development of polymeric nanogels (NGs) loaded with CDDP and coated with an anti-STn antigen–specific antibody (TKH2 monoclonal antibody) for the targeted treatment of PDAC. TKH2-functionalized, CDDP-loaded NGs delivered a significantly higher amount of platinum into the cells and tumors expressing STn antigens. We also confirmed that a synergistic cytotoxic effect of sequential exposure of pancreatic cancer cells to Gem followed by CDDP can be mimicked by the codelivery of CDDP-loaded NGs (NG/CDDP) and free Gem. In a murine orthotopic model of PDAC, combined simultaneous treatment with Gem and targeted NG/CDDP significantly attenuated tumor growth with no detectable acute toxicity. Altogether, these results suggest that combination therapy consisting of Gem followed by TKH2-conjugated CDDP NGs induces highly synergistic therapeutic efficacy against pancreatic cancer. Our results offer the basis for development of combination drug regimens using targeted nanomedicines to increase treatment effectiveness and improve outcomes of PDAC therapy.

Introduction

Pancreatic ductal adenocarcinoma (PDAC) is one of the most lethal malignancies, due to its aggressive tumorigenicity, early metastasis, and development of drug resistance to standard-care chemotherapy. PDAC is projected to become the second-leading cause of death within the next decade, with a 5-year survival rate of about 6% (Rahib et al., 2014). Since its approval in 1997, gemcitabine (Gem) has been considered the first-line treatment for advanced PDAC. However, treatment options are limited after Gem failure. The combination of Gem with cisplatin (CDDP) has been explored in clinical trials for metastatic disease. As part of the chemotherapeutic combination FOLFIRINOX (folinic acid, 5-fluorouracil, irinotecan, and oxaliplatin), platinum compounds showed significant efficacy (Conroy et al., 2011). CDDP acts by damaging the DNA. CDDP is first converted into an aqueous form within the cell by replacing the labile chloro groups with water molecules. This active form is then able to form covalently linked adducts with

This work was partly supported by the Nebraska Department of Health and Human Services [Grant LB506], the National Institutes of Health National Cancer Institute [Grants 1R01-CA208108 (to P.R.) and U01-CA198910 to (T.K.B.)], and the Nebraska Center for Nanomedicine, which is supported by the National Institutes of Health National Institute of General Medical Sciences [Institutional Development Award P20-GM103480 (to T.K.B.)].
[1]Current affiliation: Gene Therapy Development, Biogen, Cambridge, Massachusetts.
https://doi.org/10.1124/jpet.118.255372.
[S] This article has supplemental material available at jpet.aspetjournals.org.

ABBREVIATIONS: CDDP, cisplatin; CI, combination index; D_{eff}, hydrodynamic effective diameter; DMEM, Dulbecco's modified Eagle's medium; EDC, 1-(3 dimethylaminopropyl)-3-ethylcarbodiimide hydrochloride; Gem, gemcitabine; ICP-MS, inductively coupled plasma mass spectrometry; Luc, luciferase; Mal, maleimide; MTT, 3-(4,5-dimethylthiazol-2-yl)-2,5-diphenyltetrazolium bromide; NG, nanogel; PBS, phosphate-buffered saline; PDAC, pancreatic ductal adenocarcinoma; PDI, polydispersity index; PEG, polyethylene glycol; PMA, poly(methacrylic acid); SC, SimpleCell; STn, sialyl Tn; WT, wild type.

the DNA. This initial assault further activates a series of signaling pathways that ultimately lead to cell cycle arrest and apoptosis (Eastman, 1990). However, how exactly the apoptotic pathways are activated as a result of CDDP insult remains unclear. On the other hand, Gem is a deoxycytidine analog whose mechanism of activation involves conversion into a phosphorylated active form, followed by incorporation into the DNA as a false nucleotide (Hertel et al., 1988; van Moorsel et al., 1999a). Usually, another deoxynucleotide is added into the DNA before the synthesis stops. Another minor mechanism of action of Gem is its ability to inhibit ribonucleotide reductase, a key enzyme in the repair mechanism of the DNA. Many studies have reported the benefit of administration of Gem prior to that of CDDP, with the reason of increased formation of platinum-DNA adducts when the DNA has already been damaged and exposed due to the incorporation of deoxycytidine or active Gem (van Moorsel et al., 1999b). Gem in turn inhibits repair of the formed platinum-DNA adducts and reduces the efficacy of nucleotide excision repair by its ability to prevent the action of ribonucleotide reductase (Yang et al., 1995; McMahon et al., 2010). Conversely, when platinum compounds are administered prior to Gem, the formed platinum-DNA adducts can no longer allow for the incorporation of Gem, which leaves no scope for Gem to act. In this study, we show that Gem administration followed by CDDP exhibits a schedule-dependent synergistic cytotoxic activity in PDAC. However, this combination proved to be only marginally effective in actual practice due to the combined increased toxicity of both agents. We also show that encapsulation of CDDP in polymeric nanogels (NGs) with crosslinked ionic cores enhances its tumor accumulation and improves its safety profile. Furthermore, the sustained release profile of CDDP from NGs allows for the administration of free Gem and CDDP-loaded NGs in a single injection while still retaining the schedule-dependent synergy of the combination.

Monoclonal antibodies are being used in targeted therapy to deliver chemotherapeutic agents directly to cancer cells. Interestingly, overexpression of the tumor-specific carbohydrate antigen sialyl Tn (STn) has been observed in many epithelial cancers and the highest frequency was detected in PDAC. Increased expression of the STn antigen correlates with unfavorable prognosis and shorter overall patient survival. Previously, we demonstrated that aberrant expression of these immature truncated O-glycans promotes malignant features in cancer cells, such as increased migration, invasiveness, basement membrane disruption, and loss of cellular architecture (Radhakrishnan et al., 2014). Since STn has not been detected in healthy tissues (Ferreira et al., 2013; Loureiro et al., 2015) and considering its clinical relevance in human malignancies and available therapies based on this antigen, STn can be used as an important target in pancreatic cancer. Therefore, this study was designed considering the STn antigen as a target to deliver CDDP to avoid off-target accumulation of this chemotherapeutic agent and explore its activity in combination with Gem.

Materials and Methods

Reagents. Polyethylene glycol-*b*-poly(methacrylic acid) diblock copolymer (PEG_{170}-*b*-PMA_{180}, Đ = 1.45) was acquired from Polymer Source. Maleimide-PEG-amine (Mal-PEG-NH_2, 7.5 kDa) was obtained from JenKem Technology. Gem hydrochloride, CDDP, 2-iminothiolane hydrochloride, EDTA, and all other chemicals were from Sigma-Aldrich. Cell culture media (RPMI 1640 and Dulbecco's modified Eagle's medium [DMEM]) and fetal bovine serum were from Invitrogen. 3-(4,5-Dimethylthiazol-2-yl)-2,5-diphenyltetrazolium bromide (MTT) reagent was purchased from Research Products International.

Preparation of NGs. Polymeric NGs were synthesized as described previously (Kim et al., 2009). In brief, PEG_{170}-*b*-PMA_{180} chains were assembled into PEG_{170}-*b*-PMA_{180}/Ca^{2+} complexes ($[Ca^{2+}]/[COO^-]$ = 1.3 mol/mol) followed by crosslinking of the polyion chains with 1,2-ethylenediamine using 1-(3 dimethylaminopropyl)-3-ethylcarbodiimide hydrochloride (EDC) chemistry ([COOH]/[EDC] = 5; $[EDC]/[NH_2]$ = 1). The resulting NGs were purified by dialysis against water in the presence of a chelator (100 mM EDTA) and ammonia (0.5%).

CDDP Loading and Antibody Conjugation to NGs. CDDP loading was achieved as previously described (Oberoi et al., 2011). Briefly, CDDP and NGs were dissolved in water ([CDDP] = 1 mg/ml, $[CDDP]/[COO^-]$ = 0.5) and reacted for 48 hours at pH 9 and 37°C. CDDP-incorporated NGs were concentrated and washed with water separated using an Amicon Ultra-15 centrifugal filter unit (molecular mass cutoff of 30 kDa). Thiolation of the antibody (TKH2 or nonspecific IgG) was performed in phosphate buffer (pH 8, 10 mM EDTA) using 2-iminothiolane (15 Eq, 1 hour) (Steinhauser et al., 2006; Manjappa et al., 2011). The thiolated antibody was purified using a Zeba Spin desalting column previously equilibrated with 10 mM EDTA phosphate buffer, pH 7, per the manufacturer's protocol. Mal-PEG-NH_2 (10 Eq) was then added to the thiolated antibody and allowed to react for 2 hours. The excess of unreacted PEG was removed by ultrafiltration (molecular mass cutoff of 30 kDa). The PEGylated antibody was then coupled to NGs via amidation reaction with free carboxyl groups in the presence of EDC ($[COO^-]/[PEG\text{-}NH_2]$ = 1.5). The mixture was passed through a Sepharose CL-6B column to remove the unbound antibody (Nukolova et al., 2011). The resulting mixture contained both unmodified and antibody-conjugated NGs. Protein content of this mixture was determined by a microBCA assay kit (Thermo Scientific) using bovine serum albumin as the standard per the manufacturer's protocol.

Characterization of NGs. The size [hydrodynamic effective diameter (D_{eff})], polydispersity index (PDI), and ζ potential of NGs were determined by dynamic light scattering. The measurements were performed in the automatic mode at 25°C and analyzed using software provided by the manufacturer (Zetasizer; Malvern Instruments Ltd.). The reported values were based on the average of three separate measurements.

Cell Culture Conditions and Transductions. T3M4 wild-type (WT) cells with either low or no expression of STn antigen and T3M4 core 1β3-Gal-T–specific molecular chaperone knockout SimpleCell (SC) cells that aberrantly express STn antigens were maintained as previously reported (Radhakrishnan et al., 2014). The cells were transduced with firefly luciferase (Luc) and green fluorescent protein–expressing lentiviral vectors per the manufacturer's instructions (Capital Biosciences) to obtain the T3M4/Luc cell line.

NGs and CDDP Cellular Uptake. Cells (10^6 cells/well) were seeded in 24-well plates in DMEM 24 hours prior to exposure to Cy3-labeled TKH2-NG or IgG-NG (0.5 mg polymer/ml) for up to 2 hours at 37°C. Subsequently, cells were washed three times in phosphate-buffered saline (PBS), harvested with trypsin, pelleted (1500 rpm, 5 minutes), and resuspended in PBS. The fluorescence of treated cells was analyzed using Becton Dickinson FACStar Plus based on 5000 events acquired for each sample and gated to exclude debris and dead cells. To assess CDDP cellular uptake, T3M4 WT and SC cells (100,000 cells/well) were plated in a six-well plate and incubated for 2 days, followed by treatment with TKH2-NG/CDDP or IgG- NG/CDDP for 1 or 2 hours. The drug concentration during the exposure was 161.5 μM in CDDP equivalents. After incubation, cells were washed in PBS, trypsinized, pelleted by centrifugation, and digested with 0.3 ml concentrated nitric acid. Platinum concentrations were determined by inductively coupled plasma mass spectrometry (ICP-MS).

In Vitro Cytotoxic Activity. T3M4 WT and SC cells were plated at a density of 5000 cells/well in 96-well plates and incubated for 24 hours.

The cells were treated as follow; free Gem, free CDDP, Gem+CDDP, Gem (24 hours) + CDDP (24 hours), CDDP (24 hours) + Gem (24 hours), CDDP-NG, Gem + TKH2-NG/CDDP, Gem + IgG-NG/CDDP at equivalent doses of CDDP (0–10 μg/ml) or Gem (0–10 ng/ml) for a total of 48 hours in DMEM at 37°C. The CDDP/Gem molar ratio was about 1140:1 or 1000:1 w/w. Sterile Gem, CDDP, and CDDP-NG solutions were prepared in dextrose (5%) and required dilutions were made in DMEM. After incubation, each well was washed with PBS and allowed to grow in fresh DMEM for 24 hours. Cell viability was then analyzed using the MTT assay (Mosmann, 1983) and IC_{50} values of different treatments were calculated using GraphPad Prism software. The synergy, antagonism, or additive effects of the drug combination were assessed by combination index (CI) analysis using CompuSyn software based on the Chou-Talalay method (Chou, 2010).

In Vivo Orthotopic Pancreas Tumor Studies. All animal experiments were performed with protocols approved by the University of Nebraska Medical Center Institutional Animal Care and Use Committee. For this study, female nude mice (athymic nu-nu, 4 weeks old; Charles River Laboratories) were used. Animals were kept in an Association for Assessment and Accreditation of Laboratory Animal Care International–accredited facility and were quarantined for 7 days before the start of the studies. To establish the in vivo orthotopic pancreas tumor model, T3M4/Luc cells ($\sim 2.5 \times 10^5$ cells) were injected directly into the pancreas. At day 14 after cell injection, animals were randomly distributed into six groups ($n = 10$) and then treated with 5% dextrose (control group), IgG-NG/CDDP, TKH2-NG/CDDP, free Gem, or a combination of Gem with IgG-NG/CDDP or Gem with TKH2-NG/CDDP at an equivalent dose of 4 mg/kg CDDP or 20 mg/kg Gem. The formulations were administered via tail vein every fourth day for a total of four injections. Sterile Gem solutions were prepared in dextrose (5%) and used alone or in an admixture with corresponding CDDP or NG/CDDP solutions for drug combination treatment, such that the final dose volume would be 100 μl per dose. Tumor growth (bioluminescence imaging) and animal body weight were recorded every fourth day. Prior to imaging, mice were injected intraperitoneally with D-luciferin solution in sterile PBS (150 mg/kg) and anesthetized with isoflurane and then images were taken using an IVIS-200 system (Xenogen Corporation) as reported previously (Chai et al., 2013). The total bioluminescence signal in the regions of interest drawn around the whole abdomen region was quantified with IVIS software and expressed as photons per second per square centimeter per steradian. The animals were sacrificed on day 15 after commencement of the treatment. Organs and whole blood were collected for analysis and the peritoneal cavities were checked for the presence of metastasis.

Sample Preparation and Platinum Content Measurement in Tissues. ICP-MS analysis was used to quantify the total platinum content in excised tissues (tumor, kidney, spleen, liver, and lung of three mice per group). Thawed tissue samples of known weight were spiked with iridium internal standard and decomposed by wet-ashing with concentrated nitric acid (six volume equivalents) at 65°C with constant stirring overnight. The calibration range for the assay was 2–100 ng platinum/ml and necessary dilutions were made when the platinum concentration exceeded this range. The assay sensitivity was 0.8 ng platinum/ml, with variability not exceeding 5%.

Blood Chemistry and Histopathology. After the animals were sacrificed, blood was collected in heparin tubes. The levels of markers for hepatic and renal functions were determined using the Vetscan VERSUS analyzer (Abaxis). Excised tissue samples were fixed in 10% neutral buffered formalin, processed for paraffin embedding preparation of 5-μm-thick sections, and stained with hematoxylin and eosin (University of Nebraska Medical Center Tissue Sciences Facility).

Statistical Analysis. Statistical comparisons for in vitro studies were done using the *t* test. One-way ANOVA was used for analysis of the mean bioluminescence signal intensity and body weight data. Differences in tumor metastasis between groups were analyzed using the two-tailed Fisher exact test. A statistically significant difference was considered at $P < 0.05$. Statistical analysis was performed using GraphPad Prism 5 software.

Results

Schedule-Dependent Cytotoxicity of the Gem-CDDP Combination. The combination was found to be synergistic only when the T3M4 SC cells were first exposed to Gem followed by CDDP, with the CI value for this regimen being <1 (CI = 0.17). When CDDP administration was followed by Gem, the effect of the combination was antagonistic; the CI value exceeded 1 (CI = 1.98), whereas coadministration of Gem and CDDP provided a mere additive effect with a CI of ~1 (Table 1). These results indicate that a formulation approach involving immediate availability for Gem while delaying availability for CDDP would help in retaining the schedule-dependent synergy of action of the Gem-CDDP combination. To achieve this, CDDP was formulated in NGs with a sustained release profile with a targeting antibody conjugated on the surface of NGs to improve delivery of CDDP to tumor tissue. Gem would be administered as a free drug, making it available immediately for uptake upon intravenous administration.

Preparation and Characterization of CDDP-Loaded, Antibody-Conjugated NGs. NGs were produced by: 1) self-assembly of ionic block copolymer PEG_{170}-*b*-PMA_{180} in the presence of $CaCl_2$, followed by 2) crosslinking the PMA chains and 3) removal of the Ca^{2+} ions (Kim et al., 2009). Dynamic light scattering analysis revealed the formation of NGs with hydrodynamic D_{eff} diameters of ~114 nm (ζ potential = −25 mV) and a narrow size distribution (PDI < 0.1). Loading of CDDP (~25% w/w) occurs through coordination interactions of this drug with the COOH functionalities of NGs and leads to a reduction in size (D_{eff} = 93 nm) and increase in ζ potential to −14 mV. For conjugation, antibodies (either TKH2 or IgG) were first thiolated using Traut's reagent and PEGylated using Mal-PEG-NH_2. We used longer PEG chains (molecular mass = 7.5 kDa) as spacers between antibody and NG to avoid steric effects of PEG corona of NGs that can influence ligand-receptor binding. The terminal amino group of the PEG spacer was then used to conjugate the antibody to free carboxylate groups in the cores of CDDP-loaded NGs. Such a conjugation strategy is nonspecific for the site and for the number of PEG spacers conjugated per antibody molecule and leads to a mixture of NGs carrying a varying number of antibody molecules per NG as well as nonmodified NGs. Subsequently, free antibodies were separated by size exclusion chromatography using a Sepharose CL-6B column

TABLE 1

Comparison of IC_{50} values for different sequences of administration of Gem and CDDP against T3M4 SC cells as determined by the MTT assay

IC_{50} values were calculated with respect to CDDP and represent the mean ± S.D. of at least three independent experiments. The CI was calculated at IC_{50}.

Treatment Schedule[a]	IC_{50} (CI)
	$\mu g/ml$
CDDP for 24 h → Gem for 24 h	1.69 ± 0.052 (1.98)
Gem for 24 h → CDDP for 24 h	0.028 ± 0.004 (0.17)
CDDP-Gem coadministration	1.51 ± 0.15 (0.95)
CDDP	1.18 ± 0.14
Gem[b]	0.48 ± 0.03

[a]T3M4 SC cells were treated for total of 48 h.
[b]The IC_{50} value of Gem is expressed in nanograms per milliliter.

and the obtained mixture of antibody-conjugated NGs was used in further experiments. Protein content was ~65 μg/mg polymer for both antibodies, as determined by the microBCA assay. Modification of the CDDP/NG surface with either TKH2 or IgG led to an increase of the particle size (from 93 to 135 nm), although the PDI values still remained relatively low (Table 2). The ζ potential of the antibody-conjugated NGs was marginally increased compared with that for the nontargeted NGs (Table 2). The observed trend can be attributed to a shielding effect of additional PEG chains tethered to the NG surface as well as a decrease in the number of charged PMA carboxylate groups due to reaction with the PEG spacers.

Cellular Interactions of Antibody-Conjugated NGs. To analyze the binding affinity of the targeting antibody, either TKH2 or IgG was conjugated to fluorescein isothiocyanate–labeled NGs as described above and the cellular association of the NGs was estimated using flow cytometry. Both T3M4 SC (STn-positive) and T3M4 WT (STn-negative) cells were treated with fluorescein isothiocyanate–labeled TKH2-NG or IgG-NG. As shown in Fig. 1A and Supplemental Fig. 1, the uptake of TKH2-NG was significantly higher ($P < 0.01$) than IgG-NG in T3M4 SC cells, whereas the uptake for both types of NGs remained the same in T3M4 WT cells (Fig. 1B). In addition, the percentage of parent gated cells positive for TKH2-NGs was significantly increased in a time-dependent manner in T3M4 SC cells compared with T3M4 WT cells ($P < 0.05$) (Fig. 1C). We also measured the platinum content by ICP-MS in T3M4 cells that were treated with either CDDP-loaded TKH2-NG or CDDP-loaded IgG-NG. The platinum content was significantly higher in T3M4 SC cells treated with TKH2-NG compared with IgG-NG ($P < 0.05$), whereas both treatments showed similar platinum levels in the case of T3M4 WT cells (Fig. 1D).

In Vitro Cytotoxic Activity of CDDP-Loaded, Antibody-Conjugated NGs. The isogenic PDAC cells (T3M4 WT and SC) were treated with various combinations of free Gem and CDDP-loaded NGs, which were decorated with either the targeting anti-STn monoclonal antibody TKH2 or IgG as the nontargeted control. Combined treatments of Gem and CDDP formulations were substantially more effective in these cells than CDDP alone or NG/CDDP. The cytotoxic dose of CDDP in NGs was almost 40-fold lower when used in combination with Gem (Table 3). As seen with many targeted delivery systems (Desale et al., 2015), the uptake of targeted and nontargeted NGs can become practically the same over an extended period of time, given the stagnant environment of an in vitro assay. The same effect is expected to be the cause for similar IC_{50} values determined for cells treated with targeted (TKH2-CDDP/NG) or nontargeted (IgG-CDDP/NG) NGs. This trend was also seen across the STn-negative T3M4 WT cells. Notably, the synergistic cytotoxic interaction between Gem and CDDP when delivered to cells sequentially (Gem for 24 hours + CDDP for 24 hours, Table 3) was retained upon simultaneous treatment with Gem and CDDP/NGs.

TABLE 2

Physicochemical characteristics of drug-loaded NGs

D_{eff}, PDI, and ζ potential were determined in water (pH 6.5). Values are presented as the mean ± S.D. ($n = 3$).

Sample (pH 7.4)	D_{eff}	PDI	ζ Potential
	nm		*mV*
NG	114 ± 2	0.09 ± 0.02	−25.0 ± 1.8
CDDP/NG	93 ± 1	0.10 ± 0.02	−14.0 ± 1.3
TKH2-NG/CDDP	135 ± 2	0.15 ± 0.02	−9.6 ± 1.0
IgG-NG/CDDP	137 ± 1	0.14 ± 0.01	−10.7 ± 2.1

Antitumor Activity in the Orthotopic Pancreas Tumor Model. Therapeutic potential of the drug combination was tested in an orthotopic pancreatic cancer mouse model. Mice were injected with T3M4 SC/Luc cells (2.5×10^5 cells/30 μl) directly into the pancreas. Tumors were detectable from day 9 by bioluminescence imaging and treatment was started from day 14 of postimplantation of tumor cells. Tumor-bearing animals were treated via the tail vein with administration every fourth day for a total of four injections at equivalent doses of 4 mg/kg CDDP and 20 mg/kg Gem. The tumor progression for each individual treatment is shown in Fig. 2A. Monotherapy with either TKH2-NG/CDDP (targeted formulation) or Gem significantly slowed growth of the primary tumor ($P < 0.05$). Treatment with the Gem + TKH2-NG/CDDP combination further retarded tumor growth compared with Gem alone ($P < 0.05$) or TKH2-NG/CDDP ($P < 0.01$). The combination of Gem with IgG-NG/CDDP (nontargeted formulation) also led to suppression of tumor growth compared with IgG-NG/CDDP alone ($P < 0.01$) but did not exhibit better treatment efficacy compared with Gem monotherapy. Treatment with the Gem + TKH2-NG/CDDP targeted regimen displayed more pronounced tumor-suppressive effects than Gem + IgG-NG/CDDP; however, the difference did not achieve statistical significance (Fig. 2B). Furthermore, to analyze the antimetastatic potential of combination treatment, all major organs were dissected and observed for visible metastasis. Notably, peritoneal metastases were not observed in any of the animals ($n = 10$) that received the combination of both Gem and CDDP/NG, either targeted or nontargeted (Supplemental Fig. 2). In most organs, the combination treatment showed a better antimetastatic effect than monotherapies.

Platinum Content in Tumors and Other Organs. To compare the effectiveness of STn antigen–targeted drug carriers in delivering CDDP to tumors, tissues from three animals that were randomly selected from each treatment group were digested and tested for platinum content using ICP-MS. The platinum content in the tumors of animals treated with TKH2-NG/CDDP was significantly higher than that in animals treated with IgG-NG/CDDP ($P < 0.01$) irrespective of the presence of Gem (Fig. 3). An interesting observation is that the presence of Gem itself helped enhance the delivery of CDDP to the tumor tissue: higher platinum levels were detected in tumors of animals treated with Gem + TKH2-NG/CDDP versus TKH2-NG/CDDP ($P < 0.05$). Higher levels of platinum accumulation were also observed in the liver and spleen, organs of the mononuclear phagocyte system, but the effects of targeted TKH2-mediated delivery as well as overall enhanced delivery of CDDP due to the presence of Gem were observed exclusively in the tumor tissue and not in other healthy organs.

Clinical Chemistry Parameters and Toxicity Profiles. During the course of the treatment, body weights of animals were routinely monitored, and no significant changes were observed across different treatment groups (Supplemental Fig. 3). Blood collected from animals sacrificed at 72 hours after final dosing was subjected to analysis of clinical chemistry parameters indicative of renal and hepatotoxicity. As shown in Table 4, average alkaline phosphatase, alanine aminotransferase, and blood urea nitrogen values were in

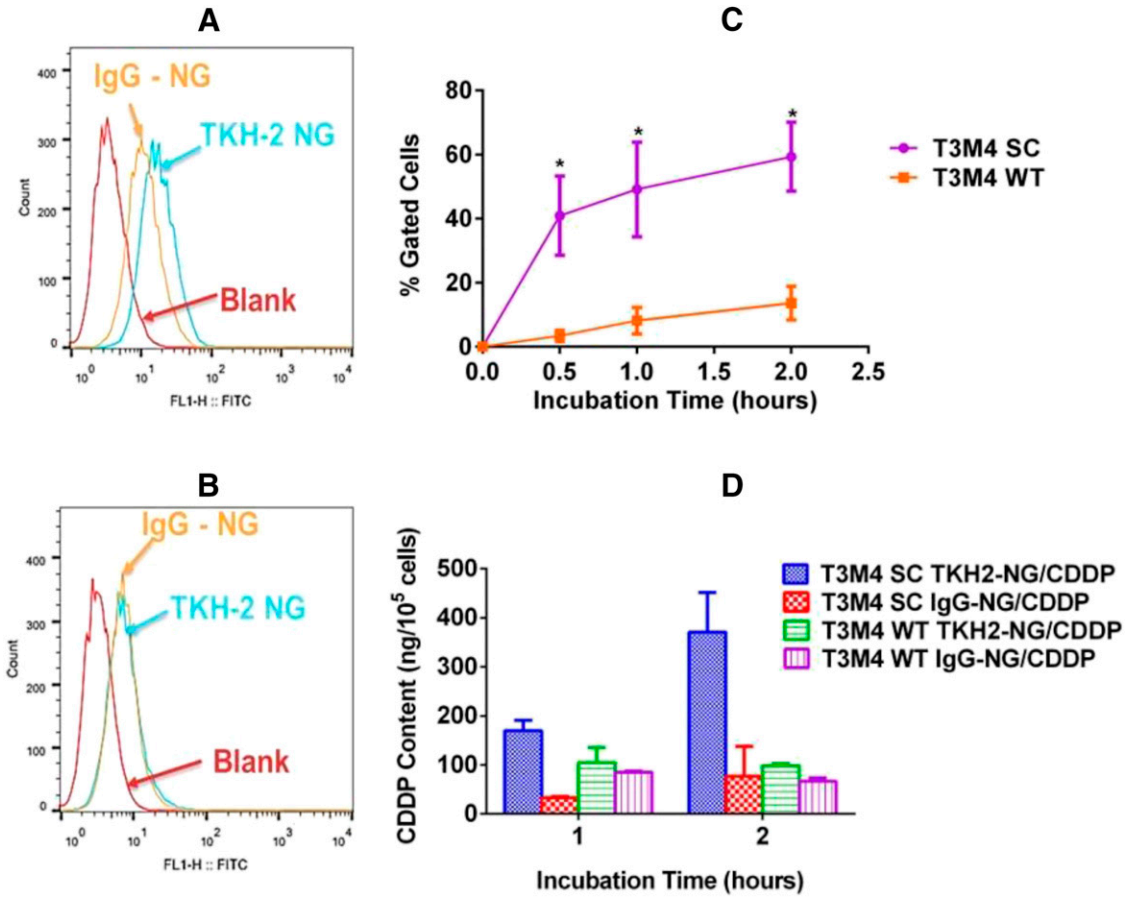

Fig. 1. (A and B) Cellular association of FITC-labeled TKH2-NG and IgG-NG with T3M4 SC cells (A) and T3M4 WT cells (B). (C) Percentage of parent gated cells as a function of time. Cells were treated with FITC-labeled TKH2-NGs at 0.5 mg/ml polymer. Protein content was 65 μg/mg polymer. *$P <$ 0.05. Data are the mean ± S.D. (n = 3). (D) Whole-cell platinum accumulation in T3M4 SC and T3M4 WT cells after incubation with TKH2-NG/CDDP or IgG-NG/CDDP (CDDP equivalent concentrations of 161.5 μM, 37°C) as measured by ICP-MS (n = 3). FITC, fluorescein isothiocyanate; FL1-H, XXX.

the normal range across all treatment groups, which indicated that no short-term toxicity to the animals occurred as a result of the treatment. Furthermore, no histopathological changes in healthy organs were seen in any of the animals, providing additional proof that all treatments were well tolerated by the animals and no short-term toxicity was evident (Supplemental Fig. 4).

Discussion

PDAC remains a major health burden, owing to its obstinate nature to therapeutic agents that impose poor prognosis of the disease. For the last 2 decades, Gem has become the reliable drug regimen for advanced PC, as it has shown significant betterment in the median overall survival of patients in clinical trials (Sinn et al., 2017; Goess and Friess, 2018). Large bodies of research evidence suggest the advantages of using combination therapy of Gem with other cytotoxic agents (Von Hoff et al., 2013; Hamada et al., 2017; Chakraborty et al., 2018; Chen et al., 2018). Although these combination therapies show significant improvement in prolongation of overall median survival in clinical trials, long-term survival of patients remains poor (American Cancer Society, 2017), demanding novel effective therapeutic approaches against disease progression. Targeted delivery of precision medicine combined with chemotherapeutic drugs is believed to improve the therapeutic effects. To address this, we have developed CDDP-encapsulated polymeric NGs conjugated with an STn antigen–specific TKH2 monoclonal antibody, which allows targeted delivery of CDDP to tumors.

In our preliminary in vitro studies, we found that administration of Gem followed by CDDP is highly effective against STn antigen–expressing PDAC cells (T3M4 SC cells) (Table 1).

TABLE 3

IC_{50} doses for drugs and drug formulations against pancreatic cancer cell lines

IC_{50} values were calculated with respect to CDDP and represent the mean ± S.D. of at least three independent experiments.

Treatment Schedule	IC_{50}	
	T3M4 SC	T3M4 WT
	$\mu g/ml$	
Gem + TKH2-NG/CDDP	0.130 ± 0.014	0.140 ± 0.003
Gem + IgG-NG/CDDP	0.150 ± 0.007	0.160 ± 0.006
Gem for 24 h + CDDP for 24 h[a]	0.030 ± 0.003	0.035 ± 0.002
Gem[b]	0.50 ± 0.03	0.80 ± 0.03
Free CDDP	1.22 ± 0.15	1.55 ± 0.04
NG/CDDP	6.45 ± 0.30	7.77 ± 0.23
Gem + CDDP coadministration	1.20 ± 0.08	1.49 ± 0.19

T3M4 (WT and SC) cells were treated with Gem, CDDP, NG/CDDP, Gem + CDDP, Gem + TKH2-NG/CDDP and Gem + IgG-NG/CDDP for 48 h and the cell viability was measured by the MTT assay.

[a]The cells were treated with free Gem for 24 h followed by the addition of CDDP and were incubated for total 48 h.

[b]IC_{50} values of Gem are expressed in nanograms per milliliters.

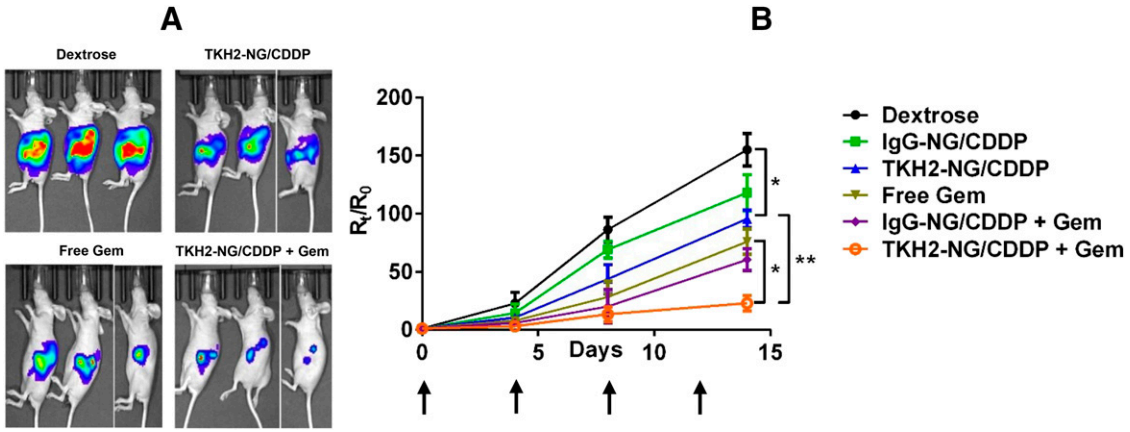

Fig. 2. In vivo antitumor efficacy of Gem + TKH2-NG/CDDP regimens in T3M4 SC/Luc orthotopic pancreatic cancer xenograft–bearing female nude mice. (A) Bioluminescence images of each of three mice representative for 10 mice per experimental arm after treatment (day 15). (B) Comparison of tumor growth inhibition after intravenous administration of 5% dextrose (control), IgG-NG/CDDP, TKH2-NG/CDDP, Gem alone, Gem + IgG-NG/CDDP, or Gem + TKH2-NG/CDDP. Drug combinations were injected in a 100 μl volume every fourth day for a total of four injections at 4 mg/kg CDDP and 20 mg/kg Gem equivalent doses (indicated by arrows). Data are presented in terms of relative bioluminescence units (R_t/R_0) to the day when treatment was initiated for the individual animal. Values indicated are the mean ± S.D. (n = 10). *$P < 0.05$; **$P < 0.01$.

We observed that the immediate availability of Gem with a delayed availability of CDDP shows a strong synergistic cytotoxic effect on T3M4 SC cells. When the drugs were applied in the reverse sequence (i.e., CDDP followed by Gem), the effect was antagonistic; simultaneous administration of the two agents showed a mere additive effect. Our data are in agreement with the previously reported synergism between Gem and platinum agents in different cancer cell lines (Huang et al., 1991; Bergman et al., 1996; van Moorsel et al., 1999a; Wang et al., 2010; Duangjai et al., 2014) when the cells were pretreated with Gem followed by platinum agents. Overall, these results highlighted the importance of sequence-specific delivery of two drugs when used in combination to achieve maximal cytotoxic effect. We previously developed a novel platform for drug delivery based on nanoscale-size polymeric NGs. The NGs are prepared through a self-assembly process, which involves formation of a crosslinked polyion core micelle coated by inert PEG chains (Bronich et al., 2005). The resulting NGs are water swollen, have very low buoyant density, and can encapsulate large amounts (~30% w/w) of water-soluble drugs through electrostatic or coordination interactions of these drugs with COOH functionalities (Kim et al., 2009; Oberoi et al., 2011). We previously demonstrated the beneficial effects of CDDP loading into the NGs as a strategy to improve pharmacokinetics and antitumor efficacy and reduce CDDP-associated nephrotoxicity in an ovarian cancer model (Oberoi et al., 2012). Moreover, the surface of NGs was decorated with various targeting ligands (small molecules, polypeptides, and antibodies) and successful delivery of targeted NGs to tumors has been confirmed (Nukolova et al., 2011, 2013).

The STn antigen is an attractive target, as its expression in normal adult tissue is rare and is largely restricted to cancer cells (Julien et al., 2012; Munkley, 2016). In this context, monoclonal antibody TKH2, which is known to bind STn antigen with high specificity, is an excellent candidate ligand to facilitate the delivery of CDDP to pancreatic cancer cells. Therein, model NGs based on the PEG-*b*-PMA copolymer were loaded with CDDP and then modified with TKH2 antibody using the bifunctional PEG linker. IgG-linked CDDP/NGs were used as a nontargeted control. The resultant NGs were about 135 nm in diameter, displayed an overall negative net charge, and were able to efficiently incorporate CDDP (loading ~25% wt.). Importantly, despite the nonspecific method of antibody conjugation to NGs that may hinder binding sites of antibody, the binding affinity of TKH2 to its target receptor was retained, which was demonstrated by a significantly higher cellular association of TKH2-NGs with cancer cells that are known to overexpress STn antigen compared with control IgG-NGs. In contrast, the uptake of both specific as well as nonspecific antibody-conjugated NGs was similar in T3M4 WT cells (Fig. 1), indicating the target specificity of TKH2 antibody against STn antigen. However, despite the enhanced cellular association of TKH2-NGs, the combination of Gem and TKH2-CDDP/NG had a lower potency compared with the free drug combination delivered to cells sequentially (Table 3). This is likely due to several factors, including: 1) lower accumulation and vesicular sequestration of CDDP/NGs in the cells compared with free drug treatment and 2) slow release of platinum species from a

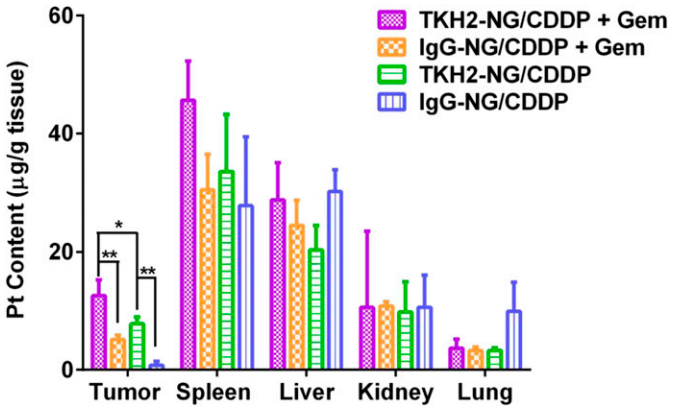

Fig. 3. Tissue distribution of platinum in different treatment groups as determined by ICP- MS. Mice were sacrificed at day 15 of the treatment with TKH2-NG/CDDP, Gem + TKH2-NG/CDDP, IgG-NG/CDDP, or Gem + IgG-NG/CDDP. Data are presented as the mean ± S.D. (n = 3). *$P < 0.05$; **$P < 0.01$. Pt, platinum.

TABLE 4
Clinical chemistry parameters as assessed by whole blood analysis from animals sacrificed on day 15
Data are presented as the mean ± S.D. (n = 3).

Treatment Group	Alkaline Phosphatase	Alanine Aminotransferase	Blood Urea Nitrogen
	IU/l		*mg/dl*
Gem + TKH2-NG/CDDP	14.5 ± 0.7	46	17
Gem + IgG-NG/CDDP	13 ± 2.65	50 ± 3	17.6 ± 1.53
TKH2-NG/CDDP	15	39.5 ± 5.5	15 ± 1.15
IgG-NG/CDDP	15	38 ± 2.6	15 ± 0.6
Free Gem	15.5 ± 2.1	45.5 ± 3	15 ± 4
Control	14 ± 0.8	46.5 ± 3.5	17 ± 2.8

nanocarrier that can lead to a reduced cytosolic drug pool. Indeed, we previously showed that the rate of release of platinum species from CDDP-loaded NGs is slow, with about 15% of platinum species released over 48 hours (Oberoi et al., 2011).

Combined Gem + TKH2-CDDP/NG therapy was further evaluated in a mouse orthotropic pancreatic cancer model. This model is known to closely mimic the tumorigenesis within the human body (Takahashi et al., 2011) and provides the ability to study site-specific dependence of therapy. To this end, T3M4 SC/Luc cells were inoculated directly into the pancreas and disease progression was monitored by non-invasive in vivo bioluminescence imaging. Treatment with the combination of Gem and targeted TKH2-NG/CDDP significantly slowed the growth of the primary pancreatic tumor (Fig. 2). This observation correlates well with the results obtained in in vitro cytotoxicity assays, wherein sequential administration of free Gem followed by free CDDP showed maximum synergy of cytotoxic activity (Table 1). In vivo, this sequential delivery is likely to be achieved by free Gem being immediately available to the tumor cells and is therefore presented first followed by CDDP that is slowly released from the NGs. Furthermore, the presence of TKH2 antibody on the surface of NGs greatly enhanced the association of the drug carrier with STn antigen–positive tumor cells (Fig. 3). Such selective binding and/or uptake of TKH2-NG/CDDP by cancer cells could result in longer retention of nanocarriers within the tumor, avoid their quick re-entry into the blood circulation, and thus offer some advantages over passively targeted formulations (Baklaushev et al., 2015). Indeed, analysis of platinum content in tumors collected 72 hours after the last injection revealed that inclusion of targeted NGs into treatment regimens led to a significantly higher tumor accumulation of platinum species compared with nontargeted NGs ($P < 0.01$). Notably, TKH2-NG/CDDP displayed significantly higher levels of platinum in tumors when it was applied in combination with Gem. Although the mechanisms underlying this phenomenon are not yet clear, recent studies in orthotopic pancreatic tumor xenografts showed increased accumulation of macrophages in tumor tissue of Gem-treated mice (Deshmukh et al., 2018). Thus, an observed elevated accumulation of platinum in tumor tissues might be facilitated through uptake of NG/CDDP by tumor-associated macrophages. Future studies will need to confirm this possibility and assess the functional consequences of our observation. The abnormal characteristics of the tumor microenvironment, such as uneven vascular distribution, heterogeneous blood flow, and elevated interstitial fluid pressure, and the tumor stromal compartment contribute to the transport barriers and compromise the ability of nanocarriers with sizes above 50 nm to penetrate through the tumor (Jain, 1990). This is especially true for poorly vascularized cancers such as PDAC (Cabral et al., 2011); therefore, the development of NG-based carriers with a size below 50 nm may further improve the delivery of platinum agents into the tumor. Furthermore, the introduction of TKH2 antibodies to NGs can also affect the pharmacokinetics, biodistribution, and tumor uptake of nanocarriers. Additional pharmacokinetic studies will be necessary to investigate the association between distribution of the targeted NGs to the tumor and the whole body and their therapeutic effect and will allow optimization of the treatment schedule for the drug combination.

Overall, our proof-of-concept studies demonstrated that TKH2-decorated NGs were effective in delivering higher payloads of CDDP to the tumor site. This led to better therapeutic efficacy of combined GEM + TKH2-NG/CDDP in terms of tumor growth retardation compared with other treatments. Collectively, these data confirm the potential of using Gem in combination with platinum-based cytotoxic agents like CDDP, the effectiveness of which can be further enhanced by using targeted delivery approaches for PDAC treatment.

Acknowledgments

We thank Ulla Mandel (Department of Cellular and Molecular Medicine, Copenhagen Center for Glycomics, University of Copenhagen, Denmark) for providing the TKH2 antibody for this study.

Authorship Contributions

Participated in research design: Hollingsworth, Radhakrishnan, Bronich.

Conducted experiments: Soni, Caffrey, Mehla, O'Connell, Radhakrishnan.

Performed data analysis: Soni, Thomas, Lei, Sagar, Lele, Radhakrishnan, Bronich.

Wrote or contributed to the writing of the manuscript: Soni, Thomas, Radhakrishnan, Bronich.

References

American Cancer Society (2017) *Cancer Facts & Figures*, pp 49–71. American Cancer Society, Atlanta, GA.

Baklaushev VP, Nukolova NN, Khalansky AS, Gurina OI, Yusubalieva GM, Grinenko NP, Gubskiy IL, Melnikov PA, Kardashova KSh, Kabanov AV, et al. (2015) Treatment of glioma by cisplatin-loaded nanogels conjugated with monoclonal antibodies against Cx43 and BSAT1. *Drug Deliv* **22**:276–285.

Bergman AM, Ruiz van Haperen VW, Veerman G, Kuiper CM, and Peters GJ (1996) Synergistic interaction between cisplatin and gemcitabine in vitro. *Clin Cancer Res* **2**:521–530.

Bronich TK, Keifer PA, Shlyakhtenko LS, and Kabanov AV (2005) Polymer micelle with cross-linked ionic core. *J Am Chem Soc* **127**:8236–8237.

Cabral H, Matsumoto Y, Mizuno K, Chen Q, Murakami M, Kimura M, Terada Y, Kano MR, Miyazono K, Uesaka M, et al. (2011) Accumulation of sub-100 nm polymeric micelles in poorly permeable tumours depends on size. *Nat Nanotechnol* **6**:815–823.

Chai MG, Kim-Fuchs C, Angst E, and Sloan EK (2013) Bioluminescent orthotopic model of pancreatic cancer progression. *J Vis Exp* 76:50395.

Chakraborty A, Dorsett KA, Trummell HQ, Yang ES, Oliver PG, Bonner JA, Buchsbaum DJ, and Bellis SL (2018) ST6Gal-I sialyltransferase promotes chemoresistance in pancreatic ductal adenocarcinoma by abrogating gemcitabine-mediated DNA damage. *J Biol Chem* **293**:984–994.
Chen L, Zhou D, Liu Z, Huang X, Liu Q, Kang Y, Chen Z, Guo Y, Zhu H, and Sun C (2018) Combination of gemcitabine and erlotinib inhibits recurrent pancreatic cancer growth in mice via the JAK-STAT pathway. *Oncol Rep* **39**:1081–1089.
Chou TC (2010) Drug combination studies and their synergy quantification using the Chou-Talalay method. *Cancer Res* **70**:440–446.
Conroy T, Desseigne F, Ychou M, Bouché O, Guimbaud R, Bécouarn Y, Adenis A, Raoul J-L, Gourgou-Bourgade S, de la Fouchardière C, et al.; Groupe Tumeurs Digestives of Unicancer; PRODIGE Intergroup (2011) FOLFIRINOX versus gemcitabine for metastatic pancreatic cancer. *N Engl J Med* **364**:1817–1825.
Desale SS, Soni KS, Romanova S, Cohen SM, and Bronich TK (2015) Targeted delivery of platinum-taxane combination therapy in ovarian cancer. *J Control Release* **220**:651–659.
Deshmukh SK, Tyagi N, Khan MA, Srivastava SK, Al-Ghadhban A, Dugger K, Carter JE, Singh S, and Singh AP (2018) Gemcitabine treatment promotes immunosuppressive microenvironment in pancreatic tumors by supporting the infiltration, growth, and polarization of macrophages. *Sci Rep* **8**:12000.
Duangjai A, Luo K, Zhou Y, Yang J, and Kopeček J (2014) Combination cytotoxicity of backbone degradable HPMA copolymer gemcitabine and platinum conjugates toward human ovarian carcinoma cells. *Eur J Pharm Biopharm* **87**:187–196.
Eastman A (1990) Activation of programmed cell death by anticancer agents: cisplatin as a model system. *Cancer Cells* **2**:275–280.
Ferreira JA, Videira PA, Lima L, Pereira S, Silva M, Carrascal M, Severino PF, Fernandes E, Almeida A, Costa C, et al. (2013) Overexpression of tumour-associated carbohydrate antigen sialyl-Tn in advanced bladder tumours. *Mol Oncol* **7**:719–731.
Goess R and Friess H (2018) A look at the progress of treating pancreatic cancer over the past 20 years. *Expert Rev Anticancer Ther* **18**:295–304.
Hamada C, Okusaka T, Ikari T, Isayama H, Furuse J, Ishii H, Nakai Y, Imai S, and Okamura S (2017) Efficacy and safety of gemcitabine plus S-1 in pancreatic cancer: a pooled analysis of individual patient data. *Br J Cancer* **116**:1544–1550.
Hertel LW, Kroin JS, Misner JW, and Tustin JM (1988) Synthesis of 2-deoxy-2,2-difluoro-D-ribose and 2-deoxy-2,2′-difluoro-D-ribofuranosyl nucleosides. *J Org Chem* **53**:2406–2409.
Huang P, Chubb S, Hertel LW, Grindey GB, and Plunkett W (1991) Action of 2′,2′-difluorodeoxycytidine on DNA synthesis. *Cancer Res* **51**:6110–6117.
Jain RK (1990) Vascular and interstitial barriers to delivery of therapeutic agents in tumors. *Cancer Metastasis Rev* **9**:253–266.
Julien S, Videira PA, and Delannoy P (2012) Sialyl-Tn in cancer: (how) did we miss the target? *Biomolecules* **2**:435–466.
Kim JO, Kabanov AV, and Bronich TK (2009) Polymer micelles with cross-linked polyanion core for delivery of a cationic drug doxorubicin. *J Control Release* **138**:197–204.
Loureiro LR, Carrascal MA, Barbas A, Ramalho JS, Novo C, Delannoy P, and Videira PA (2015) Challenges in antibody development against Tn and sialyl-Tn antigens. *Biomolecules* **5**:1783–1809.
Manjappa AS, Chaudhari KR, Venkataraju MP, Dantuluri P, Nanda B, Sidda C, Sawant KK, and Murthy RSR (2011) Antibody derivatization and conjugation strategies: application in preparation of stealth immunoliposome to target chemotherapeutics to tumor. *J Control Release* **150**:2–22.
McMahon MB, Bear MD, Kulp SK, Pennell ML, and London CA (2010) Biological activity of gemcitabine against canine osteosarcoma cell lines in vitro. *Am J Vet Res* **71**:799–808.
Mosmann T (1983) Rapid colorimetric assay for cellular growth and survival: application to proliferation and cytotoxicity assays. *J Immunol Methods* **65**:55–63.
Munkley J (2016) The role of sialyl-Tn in cancer. *Int J Mol Sci* **17**:275.
Nukolova NV, Oberoi HS, Cohen SM, Kabanov AV, and Bronich TK (2011) Folate-decorated nanogels for targeted therapy of ovarian cancer. *Biomaterials* **32**:5417–5426.
Nukolova NV, Oberoi HS, Zhao Y, Chekhonin VP, Kabanov AV, and Bronich TK (2013) LHRH-targeted nanogels as a delivery system for cisplatin to ovarian cancer. *Mol Pharm* **10**:3913–3921.
Oberoi HS, Laquer FC, Marky LA, Kabanov AV, and Bronich TK (2011) Core cross-linked block ionomer micelles as pH-responsive carriers for cis-diamminedichloroplatinum(II). *J Control Release* **153**:64–72.
Oberoi HS, Nukolova NV, Laquer FC, Poluektova LY, Huang J, Alnouti Y, Yokohira M, Arnold LL, Kabanov AV, Cohen SM, et al. (2012) Cisplatin-loaded core cross-linked micelles: comparative pharmacokinetics, antitumor activity, and toxicity in mice. *Int J Nanomedicine* **7**:2557–2571.
Radhakrishnan P, Dabelsteen S, Madsen FB, Francavilla C, Kopp KL, Steentoft C, Vakhrushev SY, Olsen JV, Hansen L, Bennett EP, et al. (2014) Immature truncated O-glycophenotype of cancer directly induces oncogenic features. *Proc Natl Acad Sci USA* **111**:E4066–E4075.
Rahib L, Smith BD, Aizenberg R, Rosenzweig AB, Fleshman JM, and Matrisian LM (2014) Projecting cancer incidence and deaths to 2030: the unexpected burden of thyroid, liver, and pancreas cancers in the United States. *Cancer Res* **74**:2913–2921.
Sinn M, Bahra M, Liersch T, Gellert K, Messmann H, Bechstein W, Waldschmidt D, Jacobasch L, Wilhelm M, Rau BM, et al. (2017) Conko-005: adjuvant chemotherapy with gemcitabine plus erlotinib versus gemcitabine alone in patients after R0 resection of pancreatic cancer: a multicenter randomized phase III trial. *J Clin Oncol* **35**:3330–3337.
Steinhauser I, Spänkuch B, Strebhardt K, and Langer K (2006) Trastuzumab-modified nanoparticles: optimisation of preparation and uptake in cancer cells. *Biomaterials* **27**:4975–4983.
Takahashi M, Hori M, Mutoh M, Wakabayashi K, and Nakagama H (2011) Experimental animal models of pancreatic carcinogenesis for prevention studies and their relevance to human disease. *Cancers (Basel)* **3**:582–602.
van Moorsel CJ, Pinedo HM, Veerman G, Bergman AM, Kuiper CM, Vermorken JB, van der Vijgh WJ, and Peters GJ (1999a) Mechanisms of synergism between cisplatin and gemcitabine in ovarian and non-small-cell lung cancer cell lines. *Br J Cancer* **80**:981–990.
van Moorsel CJ, Pinedo HM, Veerman G, Vermorken JB, Postmus PE, and Peters GJ (1999b) Scheduling of gemcitabine and cisplatin in Lewis lung tumour bearing mice. *Eur J Cancer* **35**:808–814.
Von Hoff DD, Ervin T, Arena FP, Chiorean EG, Infante J, Moore M, Seay T, Tjulandin SA, Ma WW, Saleh MN, et al. (2013) Increased survival in pancreatic cancer with nab-paclitaxel plus gemcitabine. *N Engl J Med* **369**:1691–1703.
Wang S, Zhang H, Cheng L, Evans C, and Pan C-X (2010) Analysis of the cytotoxic activity of carboplatin and gemcitabine combination. *Anticancer Res* **30**:4573–4578.
Yang L, Li L, Liu L, Keating M, and Plunkett W (1995) Gemcitabine suppresses the repair of cisplatin adducts in plasmid DNA by extracts of cisplatin-resistant human colon carcinoma cells. *Proc Am Assoc Cancer Res* **36**:357.

Address correspondence to: Dr. Prakash Radhakrishnan, Eppley Institute for Research in Cancer and Allied Diseases, Fred and Pamela Buffett Cancer Center, University of Nebraska Medical Center, 98605 Nebraska Medical Center, Omaha, NE 68198-6805. E-mail: pradhakr@unmc.edu; or Dr. Tatiana K. Bronich, Department of Pharmaceutical Sciences, Center for Drug Delivery and Nanomedicine, College of Pharmacy, University of Nebraska Medical Center, 985830 Nebraska Medical Center, Omaha, NE 68198-5830. E-mail: tbronich@unmc.edu

Polymeric Nanogel-based Treatment Regimen for Enhanced Efficacy and Sequential Administration of Synergistic Drug Combination in Pancreatic Cancer

Kruti S. Soni, Divya Thomas, Thomas Caffrey, Kamiya Mehla, Fan Lei, Kelly A O'Connell, Satish Sagar, Subodh M. Lele, Michael A Hollingsworth, Prakash Radhakrishnan* and Tatiana K. Bronich*

Department of Pharmaceutical Sciences and Center for Drug Delivery and Nanomedicine, College of Pharmacy, University of Nebraska Medical Center, 985830 Nebraska Medical Center, Omaha, NE 68198-5830, USA (KSS, FL, TKB).
Eppley Institute for Research in Cancer and Allied Diseases, Fred & Pamela Buffett Cancer Center, University of Nebraska Medical Center, 986805 Nebraska Medical Center, Omaha, NE 68198-6805, USA (DT, TC, KM, KAO, SS, MAH, PR).
Department of Pathology and Microbiology, University of Nebraska Medical Center, 983135 Nebraska Medical Center, Omaha, NE 68198-3135, USA (SML).

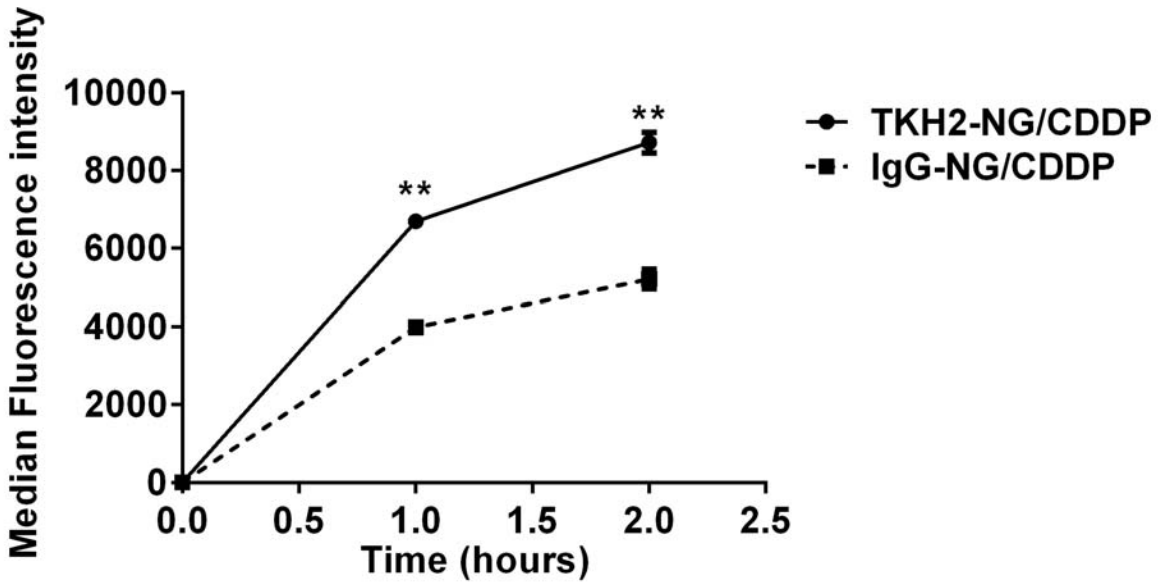

Figure S1. Cellular association of FITC-labeled TKH2 mAb – NG. Mean fluorescent intensity of FITC-conjugated TKH2 – NG and IgG – NG on T3M4 SC cells. **p < 0.01. Data are mean ± SD (n = 3).

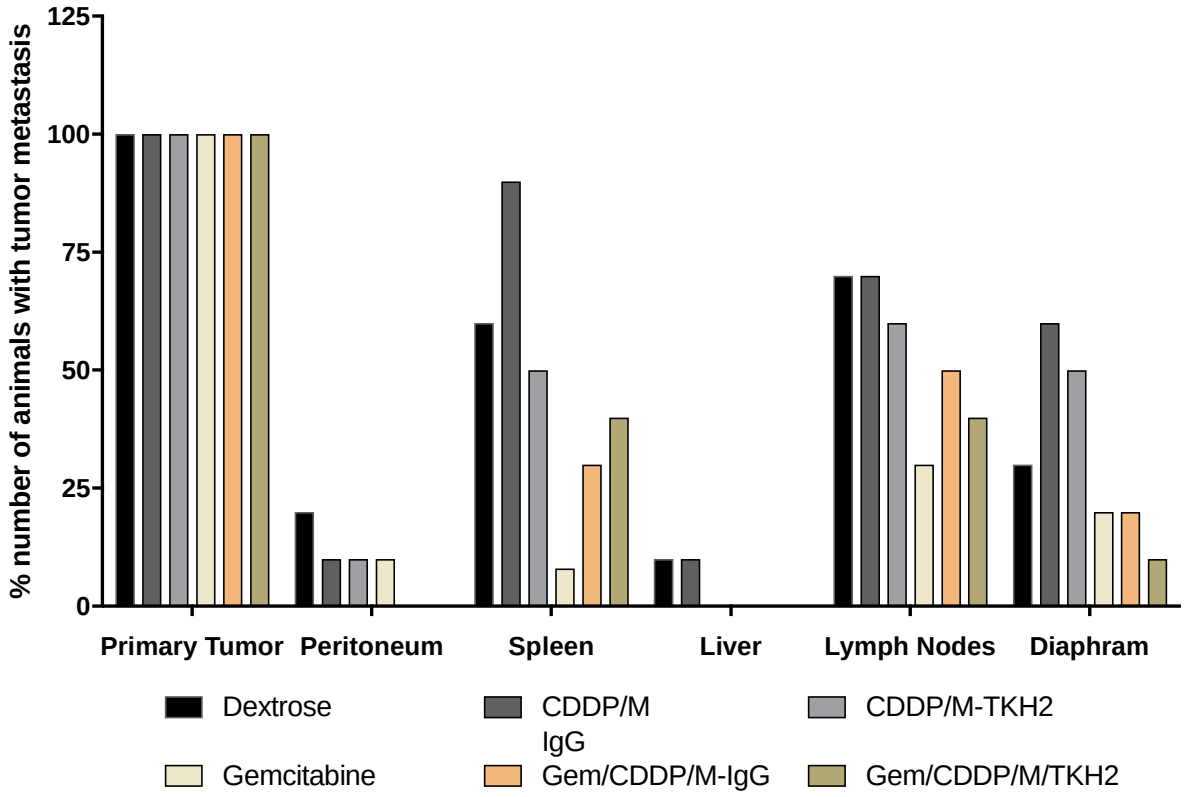

Figure S2. Incidence of primary tumor formation and metastasis as a result of various treatments. Treatment with Gem alone or Gem in combination with NG/CDDP resulted in reduced incidence of metastases in all organs and tissues but no statistical significance was reached. Importantly, no peritoneal metastasis were observed in any of the animals (n = 10) that received combination of both Gem and CDDP/NG, either targeted or non-targeted.

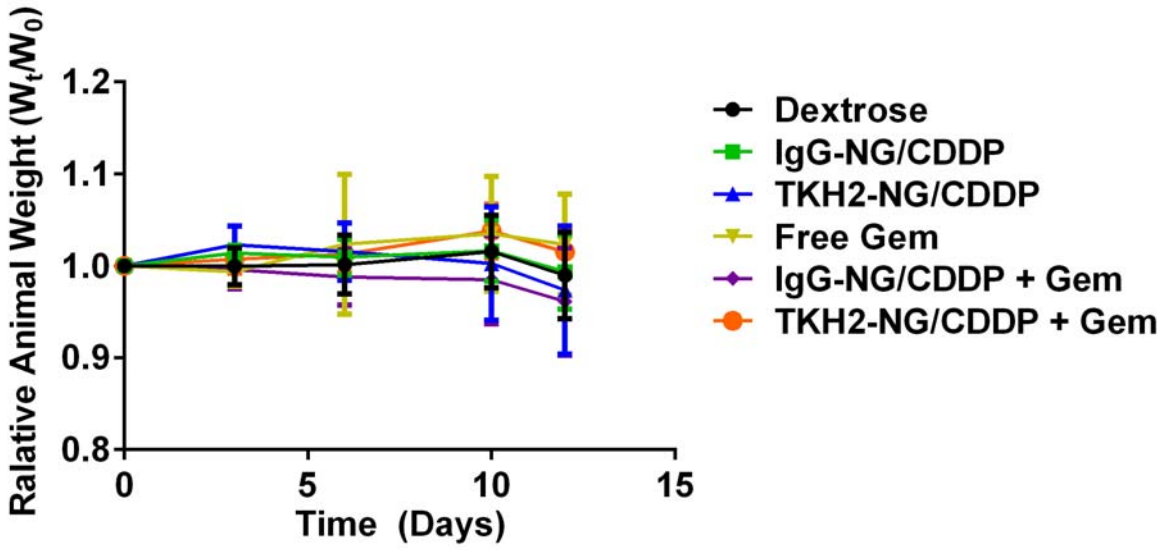

Figure S3. Relative body weight changes during the course of the study. Animals were inoculated with T3M4 SC/Luc tumor cells. Body weight was measured on days 0, 3, 6, 10 and 12. No significant change was observed in animal's body weight within the groups and between the groups at each time points.

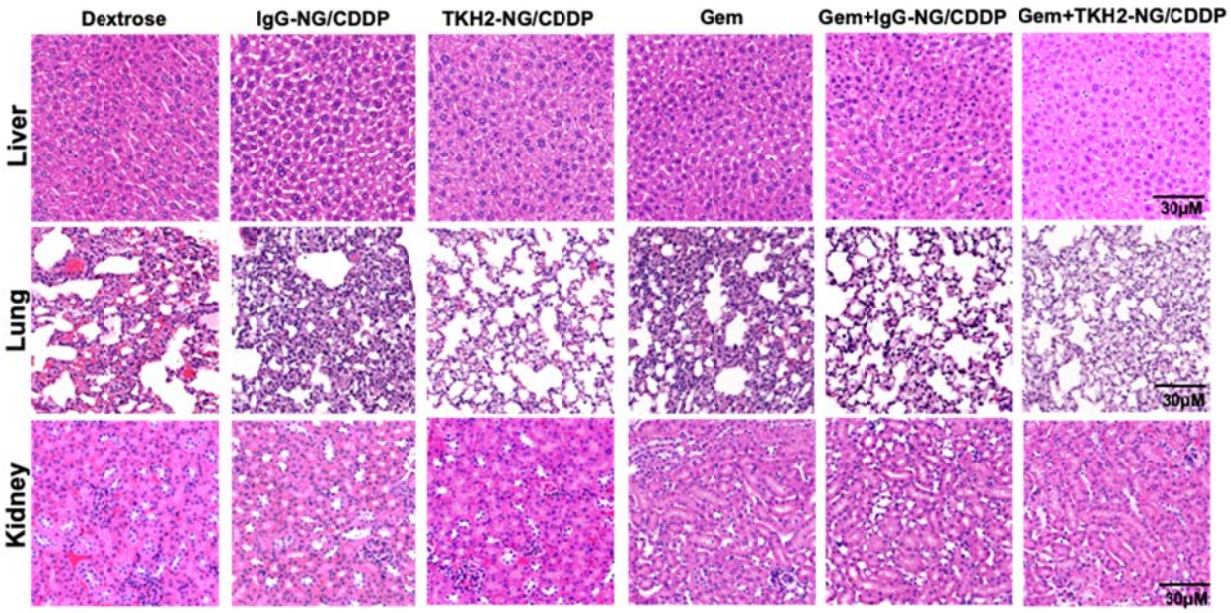

Figure S4. Vital organs like the liver, lung or kidney showed no signs of toxicity. Light microscopy images (original magnification 200×) of hematoxylin and eosin-stained tissue sections collected at the necropsy.